ORIGINAL ARTICLE

Clozapine induces astrocyte-dependent FDG-PET hypometabolism

Andréia Rocha[1] · Bruna Bellaver[1] · Débora G. Souza[1] · Guilherme Schu[1,2] · Igor C. Fontana[1] · Gianina T. Venturin[3] · Samuel Greggio[3] · Fernanda U. Fontella[1] · Manoela L. Schiavenin[1] · Luiza S. Machado[1] · Diogo Miron[4] · Jaderson C. da Costa[3] · Pedro Rosa-Neto[5,6] · Diogo O. Souza[1,7] · Luc Pellerin[8] · Eduardo R. Zimmer[1,9,10]

Abstract

Purpose Advances in functional imaging allowed us to visualize brain glucose metabolism in vivo and non-invasively with [18F]fluoro-2-deoxyglucose (FDG) positron emission tomography (PET) imaging. In the past decades, FDG-PET has been instrumental in the understanding of brain function in health and disease. The source of the FDG-PET signal has been attributed to neuronal uptake, with hypometabolism being considered as a direct index of neuronal dysfunction or death. However, other brain cells are also metabolically active, including astrocytes. Based on the astrocyte-neuron lactate shuttle hypothesis, the activation of the glutamate transporter 1 (GLT-1) acts as a trigger for glucose uptake by astrocytes. With this in mind, we investigated glucose utilization changes after pharmacologically downregulating GLT-1 with clozapine (CLO), an anti-psychotic drug.

Methods Adult male Wistar rats (control, $n = 14$; CLO, $n = 12$) received CLO ($25/35$ mg kg^{-1}) for 6 weeks. CLO effects were evaluated in vivo with FDG-PET and cortical tissue was used to evaluate glutamate uptake and GLT-1 and GLAST levels. CLO treatment effects were also assessed in cortical astrocyte cultures (glucose and glutamate uptake, GLT-1 and GLAST levels) and in cortical neuronal cultures (glucose uptake).

Results CLO markedly reduced in vivo brain glucose metabolism in several brain areas, especially in the cortex. Ex vivo analyses demonstrated decreased cortical glutamate transport along with GLT-1 mRNA and protein downregulation. In astrocyte cultures, CLO decreased GLT-1 density as well as glutamate and glucose uptake. By contrast, in cortical neuronal cultures, CLO did not affect glucose uptake.

Conclusion This work provides in vivo demonstration that GLT-1 downregulation induces astrocyte-dependent cortical FDG-PET hypometabolism—mimicking the hypometabolic signature seen in people developing dementia—and adds further evidence that astrocytes are key contributors of the FDG-PET signal.

Keywords FDG-PET · Astrocytes · GLT-1 · Glucose · Glutamate · Clozapine

Introduction

Regulation of brain glucose metabolism is key for supporting high-energy demands during neuronal firing and it involves multiple enzymes and transporters. Beyond neurons, other brain cells are also metabolically active such as the astrocytes. Indeed, astrocytes are known for their highly glycolytic metabolism (Itoh et al. 2003; Bouzier-Sore et al. 2006; Supplie et al. 2017) and positioning of their end-feet all around blood capillaries, which favors the uptake of glucose from the bloodstream (Leino et al. 1997).

Astrocytes take up glucose, via the glucose transporter 1 (GLUT1), and metabolize a substantial fraction into pyruvate through glycolysis. Then, pyruvate is converted to lactate, which is shuttled to feed neurons. This biochemical model is termed the astrocyte-to-neuron lactate shuttle (ANLS), a widely debated theoretical framework (Pellerin and Magistretti 2012; Pellerin et al. 1998; Pellerin and Magistretti 1994). The ANLS model has been corroborated by a series of in vitro and in vivo studies (Pellerin and Magistretti 1994; Takahashi et al. 1995; Pellerin and Magistretti 1997; Schurr et al. 1999; Bouzier-Sore et al. 2003; Nehlig et al. 2004; Barros et al. 2009; Chuquet et al.

This article is part of the Topical Collection on Neurology

✉ Eduardo R. Zimmer
  eduardo.zimmer@ufrgs.br

Extended author information available on the last page of the article

2010; Bittner et al. 2011; Jakoby et al. 2014). Additionally, it was observed a neuronal preference for lactate oxidation and a predominant glycolytic metabolism of glucose by astrocytes in cellular models (Itoh et al. 2003; Bouzier-Sore et al. 2006). In vivo studies have also unraveled that reduced astrocytic glutamate transport diminishes astrocyte glucose uptake (Cholet et al. 2001; Voutsinos-Porche et al. 2003). The glutamate transporter 1 (GLT-1) is the most abundant glutamate transporter in the mammalian brain, in which it has a dominant role in glutamate uptake (around 90%) (Danbolt 2001) and is predominantly located on astrocytes (Zhou and Danbolt 2013). Interestingly, glutamate transport via GLT-1 is considered as a triggering signal for glucose uptake by astrocytes (Pellerin and Magistretti 1994), this biological process being vital for brain energetics. It is important to mention that there are reports challenging the ANLS concept (Dienel 2019), which makes this topic controversial and requiring further experimental evidence.

Based on the aforementioned data, the question whether astrocyte glucose metabolism contributes to functional imaging signals, such as for positron emission tomography (PET) imaging with [^{18}F]fluoro-2-deoxyglucose (FDG) (Reivich et al. 1977; Phelps et al. 1979), has been raised. Specifically, in 1996, Pellerin and Magistretti put forward a hypothesis based on compelling evidence supporting the notion of astrocytes as contributors of FDG-PET signal (Magistretti and Pellerin 1996). In the following years, additional findings have corroborated this proposal (Magistretti and Pellerin 1999; Bonvento et al. 2002; Figley and Stroman 2011). Still, for over 40 years, the FDG-PET signal has been used as an index of neuronal activity (Sestini 2007). Recently, however, it has been demonstrated that targeting astrocytes alters the FDG-PET signal. More specifically, deletion of insulin receptors on astrocytes reduces FDG-PET signal (Garcia-Caceres et al. 2016), and activation of glutamate transport via GLT-1 on astrocytes causes widespread but graded increases in FDG-PET signal (Zimmer et al. 2017).

Recent important theoretical articles are already acknowledging the role of astrocytes in the brain FDG-PET signal (Iaccarino 2017; Zetterberg and Bendlin 2021; Perani 2019; Chetelat et al. 2020). Still, whether a reduction of glutamate uptake by astrocytes would cause in vivo FDG-PET hypometabolism—recapitulating what is seen in neurodegenerative disorders—remains unexplored. On the basis of the evidence presented above, we hypothesized that astrocyte GLT-1 downregulation would cause FDG-PET hypometabolism. To further test this hypothesis, we conducted in vivo and in vitro pharmacological challenges with CLO, a well-known anti-psychotic drug that reduces GLT-1 density (Melone et al. 2001) and glutamate transport

(Vallejo-Illarramendi et al. 2005), to assess its effects on cerebral FDG-PET signal in rats.

Materials and methods

Animals

Adult male Wistar rats, 90 days old, were maintained under a 12-h light–dark cycle (lights on at 7 A.M.), at a controlled room temperature (22 ± 1 °C) and with free access to food and water. Animals' weight was measured once a week and volume of liquid ingestion was measured three times a week.

Pharmacological treatment

Rats were randomly divided into two groups: control and CLO. Rats in the CLO group received the drug CLO (Cristália, Itapira/Brazil) in free drinking water (25–35 mg kg^{-1} day^{-1}) for 6 weeks, starting at postnatal day (PND) 91, until euthanasia. The CLO solution was prepared as previously described by Terry et al. (Terry et al. 2003). Treatment regimen, dose, and length of treatment followed the procedure described by Melone et al. (Melone et al. 2001). CLO was selected for these experiments because it specifically reduces GLT-1 (without affecting other glutamatergic transporters) (Melone et al. 2003) and substantially crosses the BBB, allowing for oral administration (Cremers et al. 2012; Naheed and Green 2001).

[^{18}F]FDG-microPET scanning

Rats were scanned longitudinally before treatment (Baseline), at PND 90, and after 6 weeks of treatment (Follow-up), at PND 136, as previously described (Bellaver et al. 2019). Briefly, after overnight fasting, animals received an intravenous injection (0.4 mL) of FDG (mean ± s.d.: 1.03 ± 0.07 mCi) into the tail vein. Then, each rat returned to its home cage for a 40-min period of awake uptake of FDG. After, they immediately underwent a 10-min static acquisition under anesthesia (2% isoflurane at 0.5 L/min oxygen flow) (see supplementary material for detailed methodology).

Metabolic networks

Cross-correlation maps were built as previously described (Bellaver et al. 2019), using a mask containing 14 volumes of interest (VOIs): left (L)-right (R) frontal cortex (FtC),

L-R temporoparietal cortex (TmPtC), L-R thalamus (Th), L-R hypothalamus (Ht), L-R striatum (St), L-R hippocampus (Hip), and L-R cerebellum (Cer). No voxel-wise network analysis was conducted due to rat brain size and PET limited resolution. Stable metabolic brain networks, using an innovative multiple sampling scheme (Schu 2021), were constructed by computing Pearson's correlation coefficients based on 2000 bootstrap samples. Graph theoretical measures such as density, global efficiency, assortativity coefficient, average degree, and average clustering coefficient were calculated for each of the bootstrap samples. Networks were corrected for multiple comparisons using the false discovery rate ($P < 0.005$) (Rubinov and Sporns 2010).

Synaptosomal preparation and L-[³H]glutamate (L-[³H]Glut) potassium-stimulated release

This procedure was performed as previously described (Almeida et al. 2017) using the whole cortex (left hemisphere) from 137 to 140 PND rats (see supplementary material for detailed methodology).

Primary cortical astrocyte cultures

Newborn (1–2 days old) male Wistar rats' cortices were aseptically resected out. The tissue was dissociated enzymatically—with trypsin 0.05% (Gibco®, Thermo Fisher Scientific) and DNase 0.003% (Sigma-Aldrich, St. Louis, MO, USA)—and mechanically (Pasteur pipet). Samples were incubated for 15 min at 37 °C for enzymatic action, followed by the addition of 10% fetal bovine serum (FBS) and centrifugation at 100 g for 5 min. Pellet was resuspended in HBSS (Gibco®) containing DNase 0.003% and centrifuged for 7 min at 100 g. The cell pellet was resuspended in DMEM (Gibco®) supplemented with 10% FBS, 15 mM HEPES, 14.3 mM $NaHCO_3$, 1% Fungizone, and 0.04% gentamicin, and plated onto 24-well plates at a density of $3–5 \times 10^5$ cells/cm^2. Cells were cultured at 37 °C in an atmosphere with 5% CO_2. The first medium exchange occurred 24 h after plating cells. The following medium changes occurred once every 4 days. After cells reached confluence, the protocol followed Vallejo-Illarramendi et al. (Vallejo-Illarramendi et al. 2005). First, 0.2 mM dibutyryl-cAMP (dBcAMP) was added for 6 days to induce GLT-1 expression. Subsequently, dBcAMP was removed and astrocytes were treated with 50 µM CLO (Sigma-Aldrich), in a medium supplemented with 1% FBS, for 48 h and used for immunofluorescence, western blot, or uptake procedures.

Primary cortical neuronal cultures

Neuronal cultures were prepared as previously described (Nunez 2008) with modifications. Newborn (0–1 day old) male Wistar rats' cortices were aseptically resected out. Tissue was dissociated enzymatically—with trypsin 0.05% (Gibco®) and DNase 0.006% (Sigma-Aldrich)—and mechanically (Pasteur pipet). Samples were incubated for 20 min at 37 °C for enzymatic action and again mechanically dissociated for 5 min. After, 20% FBS was added and samples were centrifuged at 150 g for 5 min. The pellet was resuspended in Neurobasal medium (Gibco®) supplemented with 0.5% B27 (Gibco®), 10 mM glutamine, and 0.02% penicillin/streptomycin (10,000 U/mL—Gibco®). Cells were plated at a density of $3–5 \times 10^5$ cells/cm^2 into 24-well plates pre-coated with poly-L-lysine and cultured at 37 °C in an atmosphere with 5% CO_2. Half of the medium was replaced 1 h after plating cells. Medium changes, also of half of the medium volume, occurred once every 4 days. After cells reached confluence, neurons were treated with 50 µM CLO (Sigma-Aldrich) for 48 h and used for immunofluorescence or uptake procedures.

Sodium-dependent D-[2,3-³H]-aspartate (D-[³H]Asp) uptake

D-[³H]Asp is a substrate for the high-affinity sodium-dependent glutamate transport system; therefore, its uptake was used as a proxy of glutamate uptake (Taxt and Storm-Mathisen 1984; Davies and Johnston 1976). The sodium-dependent D-[³H]Asp uptake was assessed in adult cortical slices (137–140 PND rats) incubated with 100-µM L-glutamate and in primary cultured astrocytes (P1–2 rats) incubated with 10 µM (basal) or 100 µM (stimulated) L-glutamate. The procedures followed protocols previously described (Davies and Johnston 1976; Debernardi et al. 1999) with modifications (see supplementary material for detailed methodology).

2-Deoxy-D-[³H]glucose ([³H]2DG) uptake

[³H]2DG uptake was assessed in neuronal (P0–1 rats) and astrocyte (P1–2 rats) cultures incubated with 10 µM (basal) or 100 µM (stimulated) L-glutamate. The procedures followed protocols previously described (Bellaver et al. 2019) with modifications (see supplementary material for detailed methodology).

SDS-PAGE

The whole cortex (left hemisphere) from 137 to 140 PND rats or astrocyte cultures were analyzed by SDS-PAGE,

as previously described (Bellaver et al. 2019). The following antibodies were used: GLT-1; glutamate-aspartate transporter(GLAST); Glucose transporter 1 (GLUT1); β-actin; and glyceraldehyde 3-phosphate dehydrogenase (GAPDH) (see supplementary material for detailed methodology).

RNA extraction and quantitative real-time PCR (qRT-PCR)

The whole cortex (right hemisphere) from 137 to 140 PND rats was used for the qRT-PCR analysis on which the

mRNAs of GLT-1 and GLAST were quantified as previously described (Bellaver et al. 2018) (see supplementary material for detailed methodology).

High-performance liquid chromatography (HPLC) procedures

High-performance liquid chromatography (HPLC) procedure was performed as previously described (Souza et al. 2016) using cerebrospinal fluid (CSF) to quantify three amino acids: glutamate (Glut), aspartate (Asp), and glutamine (Gln). Additionally, a HPLC with ultraviolet (UV)
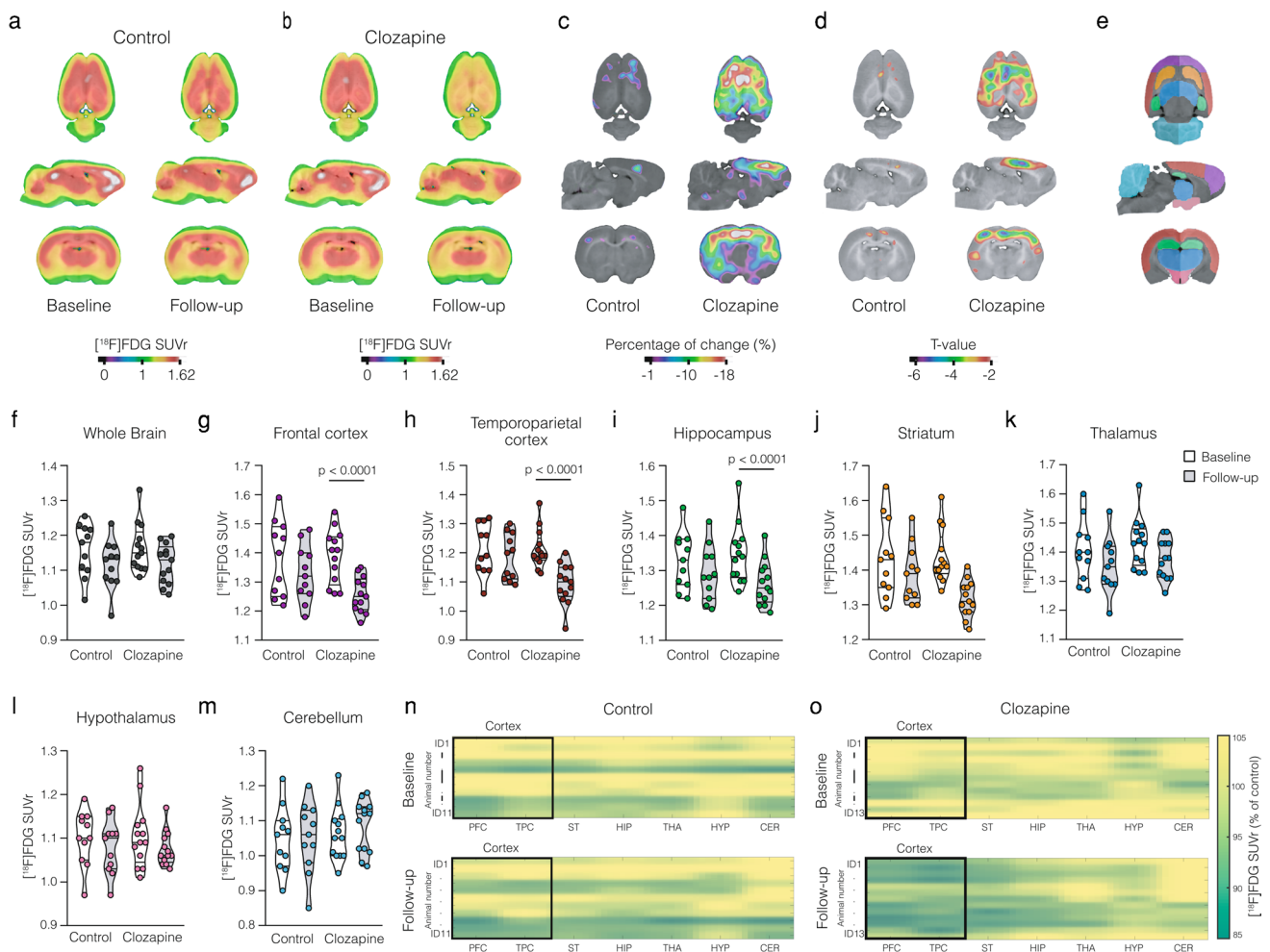

Fig. 1 Effects of CLO treatment on brain glucose metabolism assessed by [^{18}F]FDG-microPET. Brain metabolic maps showing the mean standardized uptake value reference (SUVr) of the control (a) and CLO (b) groups at Baseline and after the treatment period. Voxel-wise images representing the percentage of change difference (c) and t-statistical maps (d) between Baseline and Follow-up of control and CLO groups. Brain mask showing the volumes of interest (VOIs) (e). Control and CLO group mean regional FDG SUVr values in the whole brain (f), frontal (g) and temporoparietal cortices (h), hippocampus (i), striatum (j), thalamus (k), hypothalamus (l), and cerebellum (m) at Baseline and Follow-up. Dynamic raster plots displaying individual FDG SUVr regional means in the control (n) and CLO (o) groups. a–d Images are projected into a standard magnetic resonance imaging (MRI) in axial, sagittal, and coronal planes (control, n = 11; CLO, n = 13). Data represented as violin plots indicating the mean, interquartile range, and the minimum and maximum values. Two-way ANOVA with repeated measures, followed by Sidak's

detection method was applied to verify CLO presence and stability in the animals' drinking solution (see supplementary material for detailed methodology).

Behavioral analysis

At the end of the 6 weeks of treatment, animals were submitted to the open-field and the novel object recognition (NOR) tasks (see supplementary material for detailed methodology).

Results

CLO treatment causes brain glucose hypometabolism in vivo

The microPET analysis after CLO pharmacological intervention showed a clear FDG SUVr reduction mainly in cortical brain regions (Fig. 1a, b). Specifically, the CLO group ($n = 13$) presented a widespread FDG cortical hypometabolism, ranging from 10 to 20% (Fig. 1c). By contrast, the control group ($n = 11$) presented only a few small clusters of glucose metabolism reduction, comprising values between 1 and 6% (Fig. 1c). A voxel-wise t-statistical analysis showed a significant glucose hypometabolism mostly in the cortical regions of the CLO group, with a peak effect in the parietal cortex (peak, $t_{(23)} = 7.62$, $p < 0.0001$; Fig. 1d). On the other side, the control group presented only negligible reductions in a few isolated voxels (Fig. 1d). The two-way ANOVA of the whole brain FDG mean SUVr showed significant time effect ($p = 0.0029$; $F(1, 22) = 11.2$; Fig. 1f) but no group ($p = 0.86$; $F(1, 22) = 0.035$) or interaction ($p = 0.89$; $F(1, 22) = 0.016$), which indicates that time (Follow-up) affected the whole brain metabolism in both groups if compared to their own Baseline. A brain mask with 14 VOIs (Fig. 1e), based on the Paxinos and Watson Rat Brain Atlas, was used to obtain mean regional FDG SUVr values. In the regional analysis, a two-way ANOVA identified a significant effect of time and an interaction in the frontal cortex (time, $p < 0.0001$; interaction, $p = 0.02$; Fig. 1g), temporoparietal cortex (time, $p < 0.0001$; interaction, $p = 0.003$; Fig. 1h), and hippocampus (time, $p < 0.0001$; interaction, $p = 0.04$; Fig. 1l). The striatum (Fig. 1j) and thalamus (Fig. 1k) presented only an effect of time (striatum, $p = 0.008$; thalamus, $p = 0.007$). The hypothalamus (Fig. 1l) and cerebellum (Fig. 1m) showed no significant differences in the two-way ANOVA. Following the two-way ANOVA, Sidak's multiple comparisons test showed FDG hypometabolism in the frontal cortex ($p < 0.0001$; $t_{(22)} = 5.8$), temporoparietal cortex ($p < 0.0001$; $t_{(22)} = 6.6$), and hippocampus ($p < 0.0001$; $t_{(22)} = 5.49$) on the follow-up CLO group in comparison to

its baseline. By contrast, no regional changes were found in the control group (Baseline vs. Follow-up). The individual dynamic raster plot reinforces the observation that CLO-induced FDG hypometabolism is more pronounced in cortical areas, and that FDG metabolism remains stable in the control group (Fig. 1n, o). Furthermore, a multiple sampling scheme metabolic network analysis was performed to identify brain reorganization patterns in response to CLO. In comparison to the control group (Fig. 2a), the CLO group showed multiple altered connections within the metabolic network, presenting a widespread hyposynchronicity ($p < 0.005$, FDR-corrected, Fig. 2b). These findings were corroborated by consistent changes in graph measures, including reduced global efficiency ($p < 0.0001$, Fig. 2c), density ($p < 0.0001$, Fig. 2d), degree ($p < 0.0001$, Fig. 2e), and clustering coefficient ($p < 0.0001$, Fig. 2f). The assortativity coefficient was not significantly different between groups ($p = 0.31$, Fig. 2g).

Cortical GLT-1 and D-[3H]Asp uptake are reduced after CLO treatment

The astrocyte glutamate transporter immunocontent analysis on the cortical tissue revealed a significant reduction, around 18%, of GLT-1 levels ($p = 0.0043$; $t_{(24)} = 3.16$, Fig. 3a, b) in the CLO group (control, $n = 14$; CLO $n = 12$), but no differences on GLAST levels ($p = 0.74$; $t_{(24)} = 0.33$; Fig. 3d, e). In addition, GLT-1 mRNA expression was also reduced ($p = 0.025$; $t_{(13)} = 2.53$; control, $n = 7$ and CLO = 8; Fig. 3c). Consistently, GLAST expression was not altered ($p = 0.27$; $t_{(13)} = 1.15$; Fig. 3f). Glutamatergic transport was also evaluated by using a D-[^{3}H]Asp uptake assay on fresh cortical brain slices. The CLO group ($n = 5$) showed a significant reduction ($p = 0.048$; $t_{(9)} = 2.27$; Fig. 3g) of D-[^{3}H]Asp uptake when compared to the control group ($n = 6$). In parallel, potassium-stimulated L-[^{3}H]Glut release was assessed in synaptosomal preparations and no differences were observed ($p = 0.76$; $t_{(14)} = 0.29$; Fig. 3h). Finally, cerebrospinal fluid (CSF) levels of glutamate ($p = 0.62$; $t_{(19)} = 0.49$), aspartate ($p = 0.48$; $t_{(19)} = 0.71$), and glutamine ($p = 0.19$; $t_{(11)} = 1.38$) were not altered as well (Fig. 3i–k). Furthermore, no changes in GLUT1 immunocontent, the glucose transporter expressed in astrocytes, were identified ($p = 0.25$; $t_{(11)} = 1.20$; Supplementary Fig. 1a, b).

Effects of CLO on primary cultures of cortical astrocytes

To assess CLO-specific effects on astrocytes, we treated cortical astrocyte cultures with 50 M CLO for 48 h. Primary astrocyte cultures were immunostained with anti-GFAP (red) and DAPI (blue) (Fig. 4a). We found
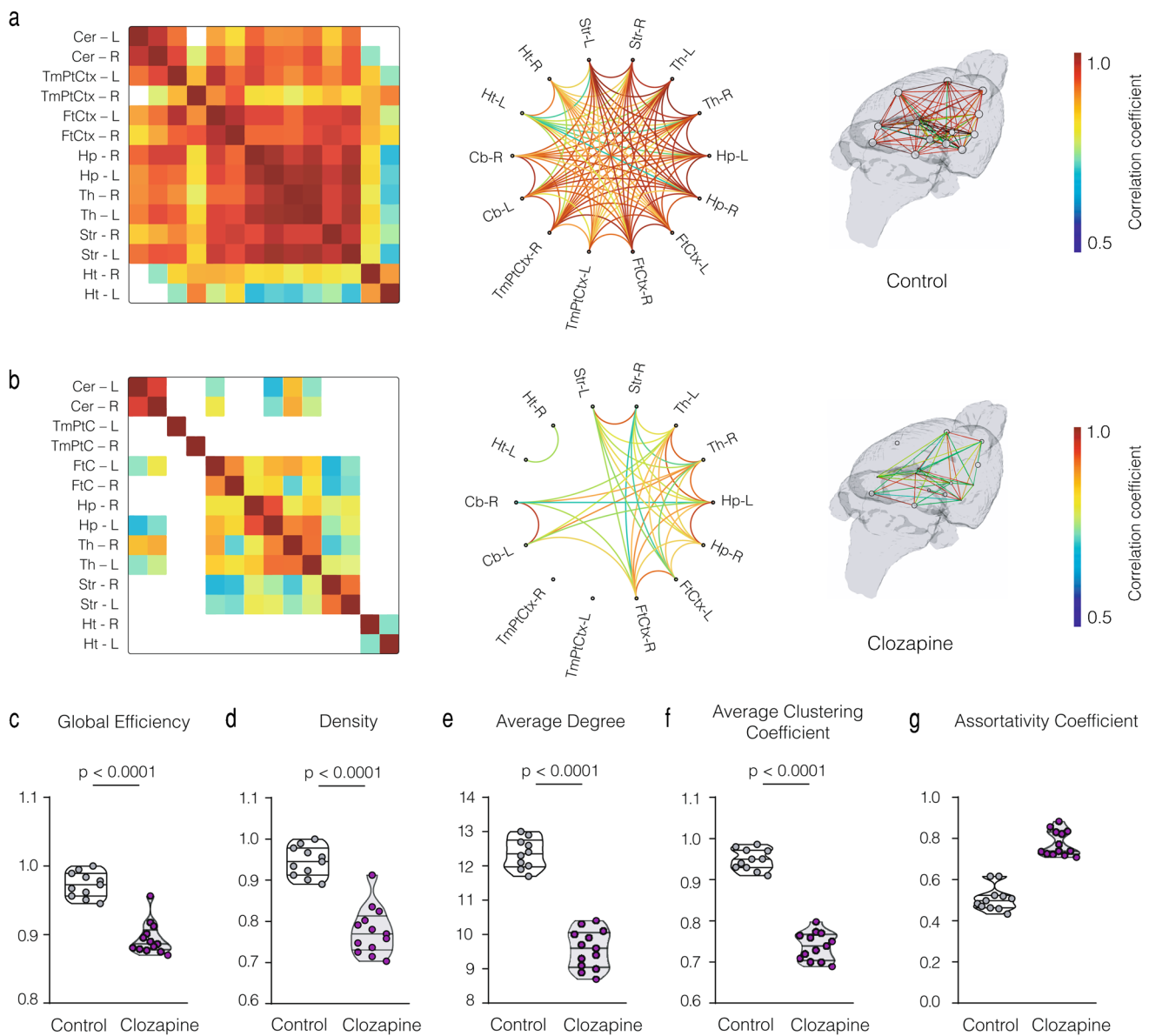
Fig. 2 [^{18}F]FDG derived metabolic networks graph measures. FDG derived metabolic networks: cross-correlation matrices (left), circular plots (middle), and brain maps (right) displaying inter-subject cross-correlation region-to-region (VOIs) associations in control (**a**) and CLO (**b**) groups at Follow-up. Data presented as correlation values with FDR-corrected threshold at $p < 0.05$. Cross-correlation matrices graph measures of global efficiency (**c**), density (**d**), average degree (**e**), average clustering coefficient (**f**), and assortativity coefficient (**g**) (control, $n = 11$; CLO, $n = 13$). Data represented as violin plots indicating the mean, interquartile range, and the minimum and maximum values. Unpaired two-tailed Student's t test

a significant decrease of GLT-1 (~ 36%, $p = 0.0019$; $t_{(7)} = 4.81$; Fig. 4b, c) and GLAST (~ 18%, $p = 0.011$; $t_{(7)} = 3.38$; Fig. 4d, e) immunocontents in the CLO group ($n = 8$, per group). In parallel, the CLO group showed a reduction of [^{3}H]D-Asp uptake in basal ($p = 0.0005$; $t_{(5)} = 7.97$; Fig. 4f) and stimulated assays ($p = 0.023$; $t_{(5)} = 3.21$; Fig. 4g). When comparing basal and stimulated [^{3}H]D-Asp uptake from control and CLO groups (Fig. 4h), we identified significant effects of treatment ($p = 0.0002$;

$F_{(1, 24)} = 18.91$) and glutamate levels ($p < 0.0001$; $F_{(1, 24)} = 48.14$) but no interaction ($p = 0.12$; $F_{(1, 24)} = 2.49$). Sidak's multiple comparisons analysis demonstrated that the control group–stimulated [^{3}H]D-Asp uptake was higher than the basal uptake for both control ($p < 0.0001$; $t_{(8)} = 5.36$) and CLO groups ($p = 0.005$; $t_{(8)} = 5.45$). In contrast, the CLO group–stimulated [^{3}H]D-Asp uptake did not differ in comparison to the basal uptake (vs. basal control, $p = 0.77$; vs. basal CLO, $p = 0.82$) and was lower than the control group–stimulated [^{3}H]D-Asp uptake ($p = 0.003$;
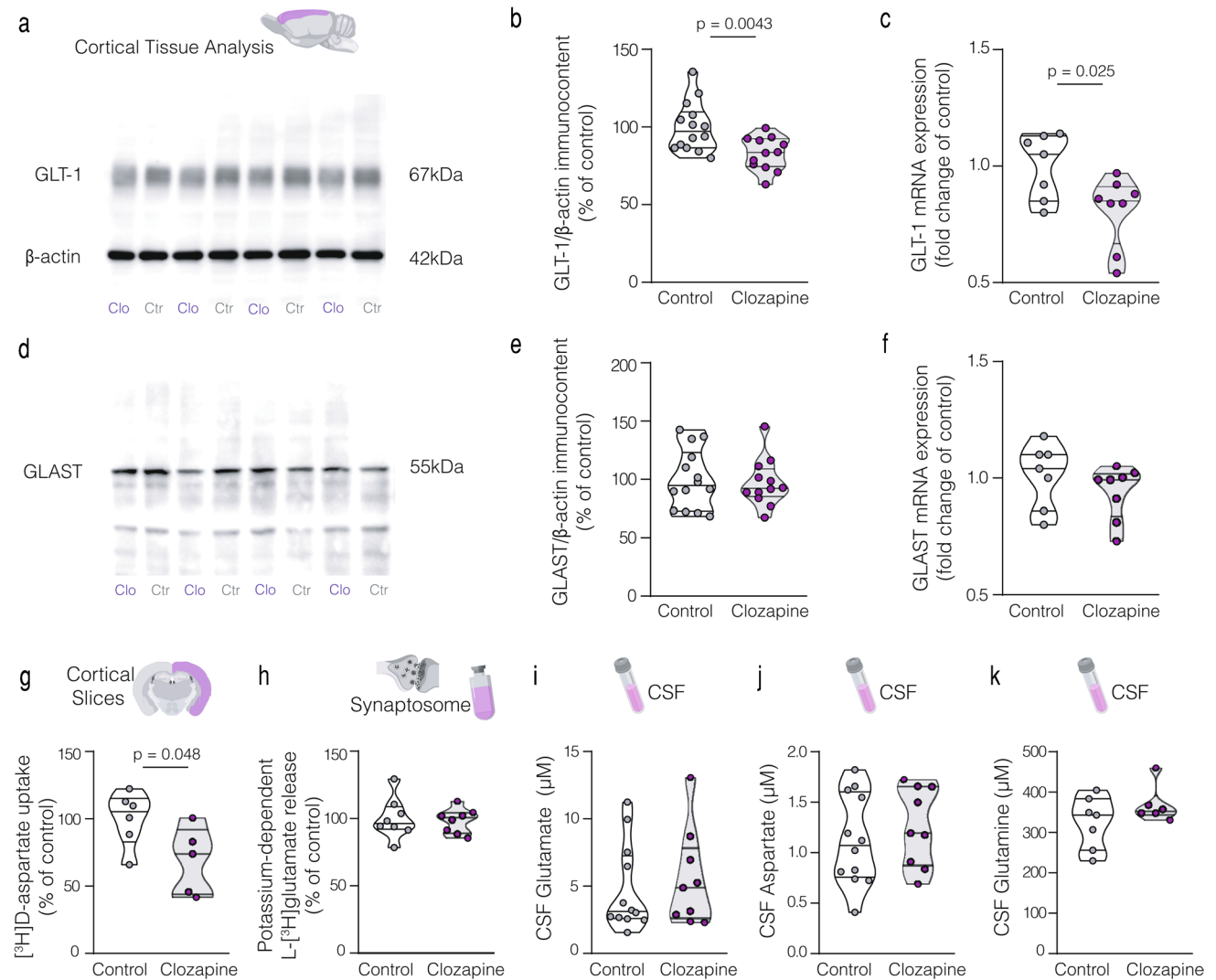
Fig. 3 Effects of CLO treatment on cortical glutamate transporter expression and activity, synaptosomal glutamate release, as well as glutamate, aspartate, and glutamine CSF levels. Cortical immunocontent (normalized by the β-actin immunocontent) of the glutamate transporters GLT-1 (**a**, **b**) and GLAST (**d**, **e**) in the control and CLO groups, after a 6-week treatment period (control, $n = 14$; CLO, $n = 12$). Cortical mRNA expression of GLT-1 (**c**) and GLAST (**f**) in the control and CLO groups, after a 6-week treatment period. PCR results are expressed as fold change in comparison to the control group (control, $n = 7$; CLO, $n = 8$). D-[³H]Asp uptake in cortical brain slices at the groups control and CLO (control, $n = 6$; CLO, $n = 5$) (**g**). L-[³H]Glut release from cortical synaptosomal preparations of control and CLO groups ($n = 8$ for each group) (**h**). Glutamate (control, $n = 12$; CLO, $n = 9$) (**i**). Aspartate (control, $n = 12$; CLO, $n = 9$) (**j**). Glutamine (control, $n = 7$; CLO, $n = 6$) (**k**) cerebrospinal fluid concentrations in control and CLO groups. Data represented as violin plots indicating the mean, interquartile range, and the minimum and maximum values. Unpaired two-tailed Student's t test

$t_{(8)} = 6.623$). Also, results of [³H]2DG uptake revealed no differences for basal uptake ($p = 0.6054$; $t_{(7)} = 0.54$; Fig. 4i) but a decrease of stimulated uptake for the CLO group ($p = 0.0002$; $t_{(7)} = 7.19$; Fig. 4j). An analysis comparing [³H]2DG uptake in these four experimental conditions (Fig. 4k) showed effects of treatment ($p < 0.0001$; $F(1, 28) = 22.54$), glutamate level ($p = 0.0061$; $F(1, 28) = 8.79$), and an interaction ($p < 0.0001$; $F(1, 28) = 21.34$). Sidak's multiple comparisons analysis demonstrated that the control group–stimulated [³H]2DG uptake was higher than the control and CLO groups in the basal condition

($p < 0.0001$). Also, the CLO group–stimulated [³H]2DG uptake was reduced if compared to the stimulated control group ($p < 0.0001$). Furthermore, no changes in the GLUT1 immunocontent were identified ($p = 0.71$; $t_{(3)} = 0.39$; Supplementary Fig. 1c, d).

Effects of CLO treatment on primary cultures of cortical neurons

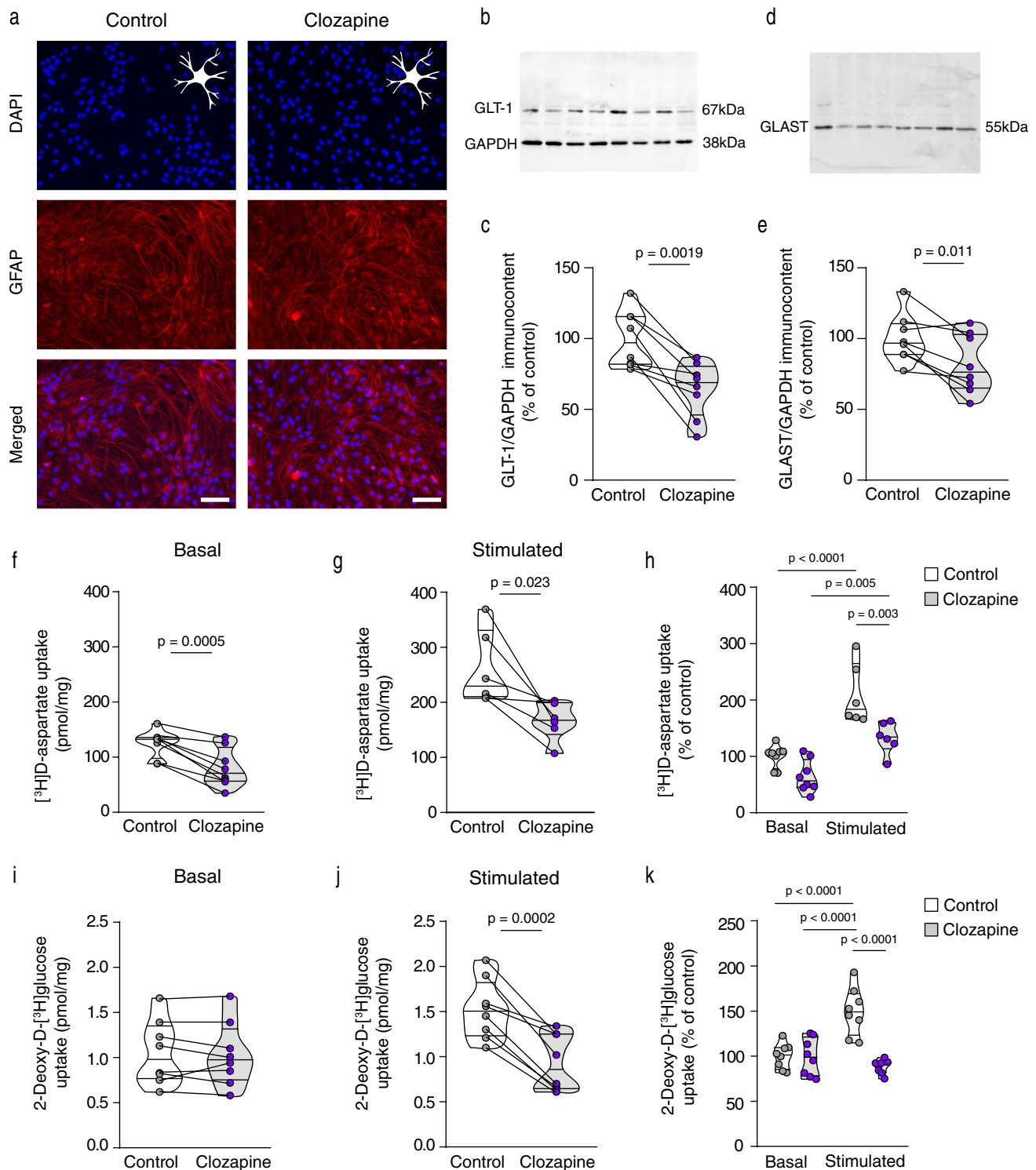Additionally, we evaluated the effect of CLO on neuronal cultures. Primary neuronal cultures were immunostained

Fig. 4 Evaluation of CLO treatment effects on [³H]D-Asp and [³H]2DG uptake in cortical astrocyte cultures. Representative images of primary cortical astrocyte cultures stained with anti-GFAP (red) and DAPI (blue); ×200 magnification and scale bar = 50 μm (**a**). Immunocontent of glutamate transporters GLT-1 (**b**, **c**) and GLAST (**d**, **e**) in primary cortical astrocyte cultures (normalized by GAPDH immunoreactivity). Basal (10 μM glutamate) (n = 6 for each group) (**f**) and stimulated (100 μM glutamate) (**g**) [³H]D-Asp uptake in astrocyte cultures. Basal (10 μM glutamate) (**i**) and stimulated (100 μM glutamate) (**j**) [³H]2DG uptake in astrocyte cultures. Comparisons of [³H]D-Asp (**h**) and [³H]2DG (**k**) uptake results in both conditions (basal and stimulated) for control and CLO groups. Uptake values expressed as percentage of control basal results (n = 8 for each group). Data represented as violin plots indicating the mean, interquartile range, and the minimum and maximum values. Paired two-tailed Student's *t* test or two-way ANOVA; two-way ANOVA followed by Sidak's
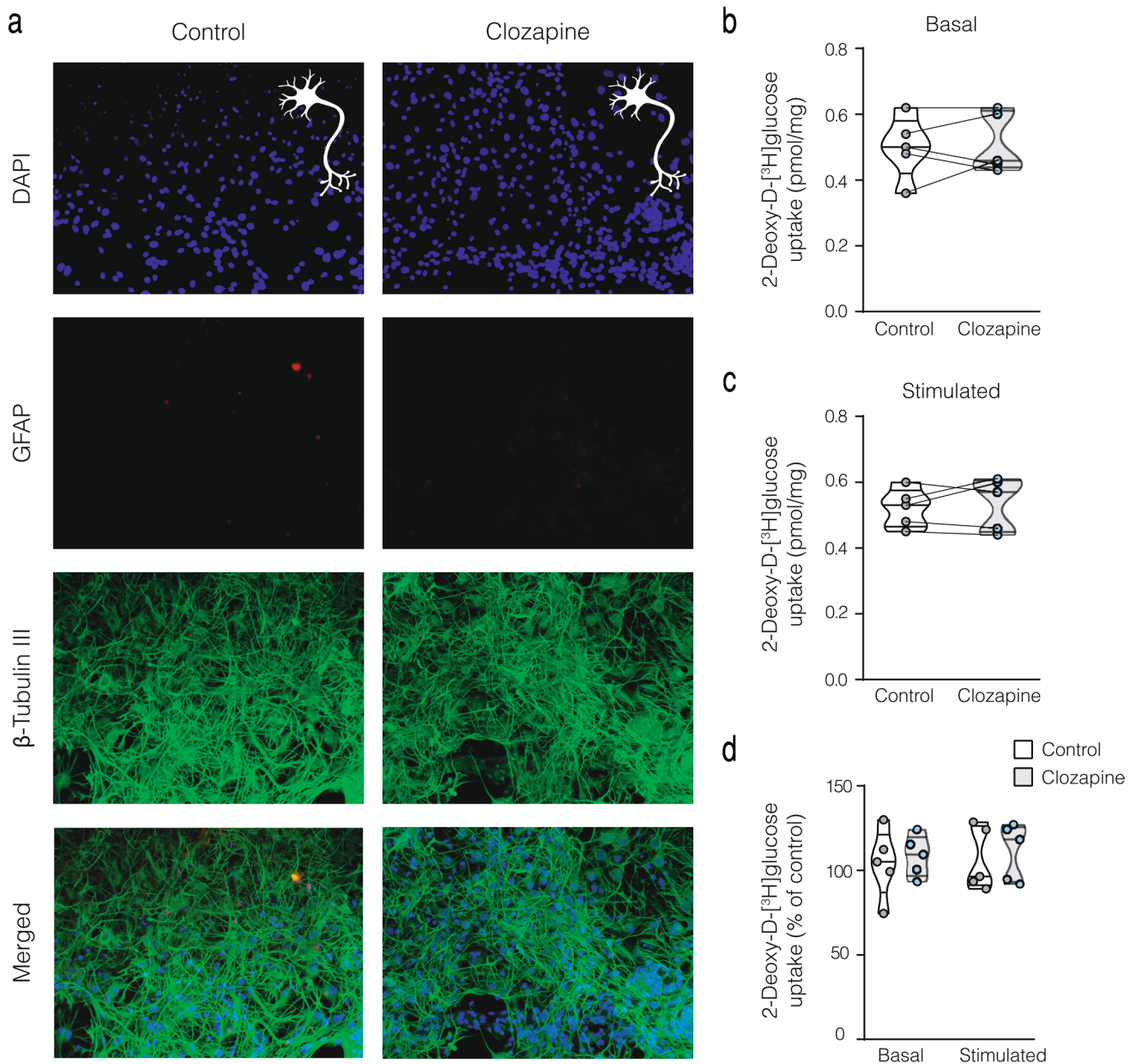
Fig. 5 Evaluation of CLO treatment effects on [³H]2DG uptake in cortical neuron cultures. Representative images of the primary cortical neuronal cultures stained with anti-GFAP (red), anti-β-Tubulin III (green), and DAPI (blue); ×100 magnification and scale bar = 100 μm (**a**). Basal (10 μM glutamate) (**b**) and stimulated (100 μM glutamate) (**c**) [³H]2DG uptake in neuronal cultures. Comparisons of [³H]2DG uptake results in both conditions (basal and stimulated) for control and CLO groups (**d**). Uptake values expressed as percentage of control basal results ($n = 5$ for each group). Data represented as violin plots indicating the mean, interquartile range, and the minimum and maximum values. Two-way ANOVA followed by Sidak's

with anti-GFAP (red), anti-β-Tubulin III (green), and DAPI (blue) (Fig. 5a). We found no differences between the control and CLO groups for [³H]2DG uptake under basal ($p = 0.70$; $t_{(4)} = 0.40$; Fig. 5b) and stimulated conditions ($p = 0.54$; $t_{(4)} = 0.66$; Fig. 5c). An analysis comparing [³H]2DG uptake in these four experimental conditions (Fig. 5d) showed no effects of treatment ($p = 0.7284$; $F(1, 16) = 0.12$), glutamate levels ($p = 0.5407$; $F(1, 16) = 0.39$), or interaction ($p = 0.9787$; $F(1, 16) = 0.0007$).

Behavioral effects and treatment measures

Total distance traveled ($p = 0.17$; $t_{(26)} = 1.42$) and total immobile time ($p = 0.13$; $t_{(26)} = 1.56$) during the open-field task were not different between groups (control,

$n = 14$; CLO, $n = 12$), therefore, suggesting no sedative side effects of CLO (Prut and Belzung 2003) (Supplementary Fig.2a–c). Analysis of the time spent exploring objects during the NOR task revealed that both groups (control, $n = 7$; CLO, $n = 5$) equally explored the two identical objects during the training session and spent more time exploring the new object during the test session (control, $p = 0.0004$; $t_{(6)} = 7.22$; CLO, $p = 0.0004$; $t_{(4)} = 10.86$), indicating no impairment of short-term recognition memory (Supplementary Fig. 2d–f). Animals' body weight was measured once a week during treatment. Results showed time effect, as animals gained weight due to age-dependent normal body growth ($p < 0.0001$; $F(7, 196) = 336.6$; Supplementary Fig. 3a), but no group effect ($p = 0.35$; $F(1, 28) = 0.89$). The liquid intake showed an increase over time ($p < 0.0001$; $F(11, 121) = 7.85$; Supplementary Fig. 3b), and a lower volume intake for the CLO group (group effect, $p = 0.036$; $F(1, 11) = 11.73$), probably due to differences in the drinking water palatability. In future experiments, the addition of small quantities of a compound such as sucrose, in order to make the drinking water containing the experimental drug more palatable, should be considered. Finally, a high-performance liquid chromatography (HPLC) analysis confirmed that the animals' drinking solution preparation was yielding the expected concentration with high reproducibility, presenting a relative standard deviation (RSD) of 1.86% (Supplementary Fig. 3c). The experimental drinking solution also showed a high stability, with no noticeable modifications of CLO concentration in a 24-h period at room temperature (Supplementary Fig. 3d).

Discussion

In this study, we demonstrated that CLO causes in vivo brain glucose hypometabolism and alters the brain metabolic network. We also found that CLO decreases GLT-1 immunocontent and mRNA expression along with functional changes, including a reduction in glutamate uptake in cortical slices, and a decline in glucose and glutamate uptake in astrocyte cortical cultures. Importantly, no differences were found in cultures of cortical neurons.

Animals treated with CLO exhibited a significant widespread reduction in FDG-PET signal in the cortex (~20%) and hippocampus. Consistently, those brain regions are the ones presenting a high content of GLT-1 (Lehre et al. 1995). Additionally, we found that CLO selectively reduced cortical GLT-1 protein levels, but did not alter GLAST levels, confirming the effect originally seen by Melone et al. (Melone et al. 2003). We also identified a reduction in cortical GLT-1 mRNA expression, suggesting that CLO may act at

the transcriptional level. In parallel, CLO reduced GLT-1 and GLAST protein levels in cortical astrocyte cultures. Quite importantly, we corroborated these findings with the functional reduction of astroglial glutamate transport, measured by D-[^{3}H]Asp uptake, in cortical slices and astrocyte primary cultures. We did not find changes in synaptosomal glutamate release from cortical preparations, or in glutamate, aspartate, and glutamine concentrations in the CSF, which suggests that the glutamate-glutamine recycling process remains functional.

The in vitro evaluation using primary astrocyte cultures treated with CLO also showed a reduction of glucose uptake, while no difference was found in cultures of cortical neurons. These results suggest that astrocytes, not neurons, are the main target cells responsible for the phenomenon observed in vivo, i.e., CLO-induced FDG-PET signal reduction. Importantly, the reduction of [^{3}H]2DG uptake by CLO in cortical astrocyte cultures was only observed when stimulated by glutamate. Astrocytes increase their glucose uptake in situations of neuronal activation (Pellerin and Magistretti 2012), i.e., during high energetic demand. Accordingly, a similar outcome was also demonstrated in vivo in a two-photon microscopy study in mice, which also showed that glucose uptake is elevated in astrocytes during activation but remains close to basal levels in neurons (Chuquet et al. 2010). Our data showing that reducing GLT-1 expression decreases activity-dependent [^{3}H]2DG accumulation is also in agreement with another study performed with GLT-1 KO mice showing that invalidation of GLT-1 prevents the whisker-stimulated increase in [^{14}C]-2-deoxyglucose accumulation in the somatosensory cortex of developing animals (Voutsinos-Porche et al. 2003).

It is important to emphasize that the FDG-PET uptake phase in our experiments was conducted in freely moving animals and, thus, the FDG-PET signal here represents glucose metabolism in an awake brain. Our present data should be also put in perspective with previous results obtained with a completely different drug. Ceftriaxone is an antibiotic that was shown to cause an increase in astrocyte GLT-1 expression and activity (Rothstein et al. 2005). Treatment of primary cultures of cortical astrocytes with ceftriaxone was shown to enhance both glutamate transport and glutamate-stimulated glucose uptake through its effect on GLT-1 (Zimmer et al. 2017). But quite strikingly, ceftriaxone increased brain FDG-PET signal in rats proportionately to the density of GLT-1 expression in different brain regions (Zimmer et al. 2017). These results are simply a mirror image of the data obtained with CLO. Altogether, results with CLO and ceftriaxone reinforce the notion that astrocytes, through glutamate-stimulated glucose uptake, represent an important source of the FDG-PET signal in vivo, as postulated exactly 25 years ago (Magistretti and Pellerin 1996). Additionally, a recent study demonstrated that the modulation of microglial

cells also contributes to the FDG-PET signal (Xiang 2021). Since microglial cells account for less than 10% of brain cells in mammals, the microglia-induced effect on FDG-PET probably has the astrocytic and/or the neuronal compartment as the cellular source. In fact, it was previously demonstrated that Il-1α, IL-1β, and TNFα, classically secreted by activated microglia, enhance glucose uptake in astrocytes (Gavillet et al. 2008).

Besides its effects on glutamate transport presented above, it is also known that CLO interacts with serotonin, muscarinic, dopamine, and histamine receptors (Miyamoto et al. 2005; Stepnicki 2018). However, the direct contribution of these neurotransmission systems to brain energetics is small (Sibson et al. 1998; Scremin and Jenden 1993). Therefore, it is very unlikely that changes in glucose uptake result from these interactions. In fact, there are several studies showing that brain energy metabolism is driven predominantly by glutamatergic and, to a minor extent, GABAergic systems (for review, see (Rothman et al. 1999; Rothman et al. 2003)), with contributions of other neurotransmitters being so small that it can be disregarded in the overall scenario. However, we could not ignore the possibility of a modulatory effect on neuronal metabolism. To rule out a direct effect on neuronal energy metabolism, we tested CLO impact on neuronal cortical cultures under resting and stimulated conditions. Clearly, CLO did not change neuronal glucose metabolism in both situations, thus, strengthening the conclusion of astrocytes being at the origin of the observed hypometabolism. It is important to mention that cortical FDG-PET hypometabolism is a signature of neurodegenerative disorders such as Alzheimer's disease and frontotemporal dementia, which is interpreted as an index of neurodegeneration (Chetelat et al. 2020). Since CLO does not induce neuronal death (Chen and Nasrallah 2019; Lundberg 2020; Bastianetto et al. 2006; Stanisavljevic et al. 2019), one could argue we recapitulated cortical FDG-PET hypometabolism seen in people with dementia by only reducing glutamate transport in astrocytes.

A potential limitation to this conclusion would pertain to behavioral changes such as sedation or freezing that could have contributed to the effects observed with CLO and might jeopardize our interpretation of the cellular origin of the FDG-PET signal (Berti et al. 2014). However, we did not observe changes either in the open-field task or in a more complex behavioral task such as the NOR. Thus, it seems that CLO-induced FDG hypometabolism is not related to major behavioral changes.

In summary, our results provide microPET evidence that a treatment with CLO causes a reduction in FDG-PET signal. Primary culture data indicate that astrocytes, not neurons, are the cells responsible for this phenomenon. These results corroborate the notion that the FDG-PET signal might reflect not only neuronal activity but also astrocyte metabolism. These findings reinforce the need for a renewed interpretation of FDG-PET data in brain imaging studies. Finally, from a clinical perspective, CLO is an important anti-psychotic drug widely used in patients with schizophrenia who are either intolerant or refractory to classical neuroleptics (Conley and Kelly 2001). CLO mechanisms of action are yet not fully understood; therefore, the effect on brain energetics observed in our study might be of importance and should be better studied in this perspective. As a matter of fact, a FDG-PET hypometabolism in the frontal cortex of CLO-responsive patients has been reported a few years ago (Cohen et al. 1997; Molina et al. 2007; Molina et al. 2005). We believe this phenomenon deserves further investigation in clinical research.

Declarations

References

Itoh Y, Esaki T, Shimoji K, Cook M, Law MJ, Kaufman E, et al. Dichloroacetate effects on glucose and lactate oxidation by neurons and astroglia in vitro and on glucose utilization by brain in vivo. Proc Natl Acad Sci USA. 2003;100:4879–84. https://doi.org/10.1073/pnas.0831078100.

Bouzier-Sore AK, Voisin P, Bouchaud V, Bezancon E, Franconi JM, Pellerin L. Competition between glucose and lactate as oxidative energy substrates in both neurons and astrocytes: a comparative NMR study. Eur J Neurosci. 2006;24:1687–94. https://doi.org/10.1111/j.1460-9568.2006.05056.x.

Supplie LM, Duking T, Campbell G, Diaz F, Moraes CT, Gotz M, et al. Respiration-deficient astrocytes survive as glycolytic cells in vivo. The Journal of neuroscience : the official journal of the Society for Neuroscience. 2017;37:4231–42. https://doi.org/10.1523/JNEUROSCI.0756-16.2017.

Leino RL, Gerhart DZ, van Bueren AM, McCall AL, Drewes LR. Ultrastructural localization of GLUT 1 and GLUT 3 glucose transporters in rat brain. J Neurosci Res. 1997;49:617–26. https://doi.org/10.1002/(SICI)1097-4547(19970901)49:5%3c617::AID-JNR7%3e3.0.CO;2-S.

Pellerin L, Magistretti PJ. Sweet sixteen for ANLS. J Cereb Blood Flow Metab. 2012;32:1152–66. https://doi.org/10.1038/jcbfm.2011.149.

Pellerin L, Pellegri G, Bittar PG, Charnay Y, Bouras C, Martin JL, et al. Evidence supporting the existence of an activity-dependent astrocyte-neuron lactate shuttle. Dev Neurosci. 1998;20:291–9.

Pellerin L, Magistretti PJ. Glutamate uptake into astrocytes stimulates aerobic glycolysis: a mechanism coupling neuronal activity to glucose utilization. Proc Natl Acad Sci USA. 1994;91:10625–9. https://doi.org/10.1073/pnas.91.22.10625.

Takahashi S, Driscoll BF, Law MJ, Sokoloff L. Role of sodium and potassium ions in regulation of glucose metabolism in cultured astroglia. Proc Natl Acad Sci USA. 1995;92:4616–20.

Pellerin L, Magistretti PJ. Glutamate uptake stimulates Na+, K+-ATPase activity in astrocytes via activation of a distinct subunit highly sensitive to ouabain. J Neurochem. 1997;69:2132–7. https://doi.org/10.1046/j.1471-4159.1997.69052132.x.

Schurr A, Miller JJ, Payne RS, Rigor BM. An increase in lactate output by brain tissue serves to meet the energy needs of glutamate-activated neurons. The Journal of neuroscience : the official journal of the Society for Neuroscience. 1999;19:34–9.

Bouzier-Sore AK, Voisin P, Canioni P, Magistretti PJ, Pellerin L. Lactate is a preferential oxidative energy substrate over glucose for neurons in culture. Journal of cerebral blood flow and metabolism : official journal of the International Society of Cerebral Blood Flow and Metabolism. 2003;23:1298–306. https://doi.org/10.1097/01.WCB.0000091761.61714.25.

Nehlig A, Wittendorp-Rechenmann E, Lam CD. Selective uptake of [14C]2-deoxyglucose by neurons and astrocytes: high-resolution microautoradiographic imaging by cellular 14C-trajectography combined with immunohistochemistry. Journal of cerebral blood flow and metabolism : official journal of the International Society of Cerebral Blood Flow and Metabolism. 2004;24:1004–14. https://doi.org/10.1097/01.WCB.0000128533.84196.D8.

Barros LF, Courjaret R, Jakoby P, Loaiza A, Lohr C, Deitmer JW. Preferential transport and metabolism of glucose in Bergmann glia over Purkinje cells: a multiphoton study of cerebellar slices. Glia. 2009;57:962–70. https://doi.org/10.1002/glia.20820.

Chuquet J, Quilichini P, Nimchinsky EA, Buzsaki G. Predominant enhancement of glucose uptake in astrocytes versus neurons during activation of the somatosensory cortex. The Journal of neuroscience : the official journal of the Society for Neuroscience.

2010;30:15298–303. https://doi.org/10.1523/JNEUROSCI.0762-10.2010.

Bittner CX, Valdebenito R, Ruminot I, Loaiza A, Larenas V, Sotelo-Hitschfeld T, et al. Fast and reversible stimulation of astrocytic glycolysis by K+ and a delayed and persistent effect of glutamate. The Journal of neuroscience : the official journal of the Society for Neuroscience. 2011;31:4709–13. https://doi.org/10.1523/JNEUROSCI.5311-10.2011.

Jakoby P, Schmidt E, Ruminot I, Gutierrez R, Barros LF, Deitmer JW. Higher transport and metabolism of glucose in astrocytes compared with neurons: a multiphoton study of hippocampal and cerebellar tissue slices. Cereb Cortex. 2014;24:222–31. https://doi.org/10.1093/cercor/bhs309.

Cholet N, Pellerin L, Welker E, Lacombe P, Seylaz J, Magistretti P, et al. Local injection of antisense oligonucleotides targeted to the glial glutamate transporter GLAST decreases the metabolic response to somatosensory activation. Journal of cerebral blood flow and metabolism : official journal of the International Society of Cerebral Blood Flow and Metabolism. 2001;21:404–12. https://doi.org/10.1097/00004647-200104000-00009.

Voutsinos-Porche B, Bonvento G, Tanaka K, Steiner P, Welker E, Chatton JY, et al. Glial glutamate transporters mediate a functional metabolic crosstalk between neurons and astrocytes in the mouse developing cortex. Neuron. 2003;37:275–86. https://doi.org/10.1016/s0896-6273(02)01170-4.

Danbolt NC. Glutamate uptake. Prog Neurobiol. 2001;65:1–105.

Zhou Y, Danbolt NC. GABA and glutamate transporters in brain. Front Endocrinol. 2013;4:165. https://doi.org/10.3389/fendo.2013.00165.

Dienel GA. Brain glucose metabolism: integration of energetics with function. Physiol Rev. 2019;99:949–1045. https://doi.org/10.1152/physrev.00062.2017.

Reivich M, Kuhl D, Wolf A, Greenberg J, Phelps M, Ido T, et al. Measurement of local cerebral glucose metabolism in man with 18F-2-fluoro-2-deoxy-d-glucose. Acta Neurol Scand Suppl. 1977;64:190–1.

Phelps ME, Huang SC, Hoffman EJ, Selin C, Sokoloff L, Kuhl DE. Tomographic measurement of local cerebral glucose metabolic rate in humans with (F-18)2-fluoro-2-deoxy-D-glucose: validation of method. Ann Neurol. 1979;6:371–88. https://doi.org/10.1002/ana.410060502.

Magistretti PJ, Pellerin L. The contribution of astrocytes to the 18F-2-deoxyglucose signal in PET activation studies. Mol Psychiatry. 1996;1:445–52.

Magistretti PJ, Pellerin L. Cellular mechanisms of brain energy metabolism and their relevance to functional brain imaging. Philos Trans R Soc Lond B Biol Sci. 1999;354:1155–63. https://doi.org/10.1098/rstb.1999.0471.

Bonvento G, Sibson N, Pellerin L. Does glutamate image your thoughts? Trends Neurosci. 2002;25:359–64. https://doi.org/10.1016/s0166-2236(02)02168-9.

Figley CR, Stroman PW. The role(s) of astrocytes and astrocyte activity in neurometabolism, neurovascular coupling, and the production of functional neuroimaging signals. Eur J Neurosci. 2011;33:577–88. https://doi.org/10.1111/j.1460-9568.2010.07584.x.

Sestini S. The neural basis of functional neuroimaging signal with positron and single-photon emission tomography. Cellular and molecular life sciences : CMLS. 2007;64:1778–84. https://doi.org/10.1007/s00018-007-7056-4.

Garcia-Caceres C, Quarta C, Varela L, Gao Y, Gruber T, Legutko B, et al. Astrocytic insulin signaling couples brain glucose uptake with nutrient availability. Cell. 2016;166:867–80. https://doi.org/10.1016/j.cell.2016.07.028.

Zimmer ER, Parent MJ, Souza DG, Leuzy A, Lecrux C, Kim HI, et al. [18F]FDG PET signal is driven by astroglial glutamate transport. Nat Neurosci. 2017;20:393–5. https://doi.org/10.1038/nn.4492.

Iaccarino L, Sala A, Caminiti SP, Perani D. The emerging role of PET imaging in dementia. F1000Res. 2017;6:1830. doi:https://doi.org/10.12688/f1000research.11603.1.

Zetterberg H, Bendlin BB. Biomarkers for Alzheimer's disease-preparing for a new era of disease-modifying therapies. Mol Psychiatry. 2021;26:296–308. https://doi.org/10.1038/s41380-020-0721-9.

Perani D, Iaccarino L, Jacobs AH, Group IBIW. Application of advanced brain positron emission tomography-based molecular imaging for a biological framework in neurodegenerative proteinopathies. Alzheimers Dement (Amst). 2019;11:327–32. https://doi.org/10.1016/j.dadm.2019.02.004.

Chetelat G, Arbizu J, Barthel H, Garibotto V, Law I, Morbelli S, et al. Amyloid-PET and (18)F-FDG-PET in the diagnostic investigation of Alzheimer's disease and other dementias. The Lancet Neurology. 2020;19:951–62. https://doi.org/10.1016/S1474-4422(20)30314-8.

Melone M, Vitellaro-Zuccarello L, Vallejo-Illarramendi A, Perez-Samartin A, Matute C, Cozzi A, et al. The expression of glutamate transporter GLT-1 in the rat cerebral cortex is down-regulated by the antipsychotic drug clozapine. Mol Psychiatry. 2001;6:380–6. https://doi.org/10.1038/sj.mp.4000880.

Vallejo-Illarramendi A, Torres-Ramos M, Melone M, Conti F, Matute C. Clozapine reduces GLT-1 expression and glutamate uptake in astrocyte cultures. Glia. 2005;50:276–9. https://doi.org/10.1002/glia.20172.

Terry AV Jr, Hill WD, Parikh V, Waller JL, Evans DR, Mahadik SP. Differential effects of haloperidol, risperidone, and clozapine exposure on cholinergic markers and spatial learning performance in rats. Neuropsychopharmacology : official publication of the American College of Neuropsychopharmacology. 2003;28:300–9. https://doi.org/10.1038/sj.npp.1300039.

Melone M, Bragina L, Conti F. Clozapine-induced reduction of glutamate transport in the frontal cortex is not mediated by GLAST and EAAC1. Mol Psychiatry. 2003;8:12–3. https://doi.org/10.1038/sj.mp.4001193.

Cremers TI, Flik G, Hofland C, Stratford RE Jr. Microdialysis evaluation of clozapine and N-desmethylclozapine pharmacokinetics in rat brain. Drug metabolism and disposition: the biological fate of chemicals. 2012;40:1909–16. https://doi.org/10.1124/dmd.112.045682.

Naheed M, Green B. Focus on clozapine. Curr Med Res Opin. 2001;17:223–9. https://doi.org/10.1185/0300799039117069.

Bellaver B, Rocha AS, Souza DG, Leffa DT, De Bastiani MA, Schu G, et al. Activated peripheral blood mononuclear cell mediators trigger astrocyte reactivity. Brain Behav Immun. 2019;80:879–88. https://doi.org/10.1016/j.bbi.2019.05.041.

Schu G, Brum WS, Rodrigues YE, Cesar de Azeredo J, Pascoal TA, Benedet AL, et al. Stable brain PET metabolic networks using a multiple sampling scheme. bioRxiv. 2021:2021.03.16.435674. doi:https://doi.org/10.1101/2021.03.16.435674.

Rubinov M, Sporns O. Complex network measures of brain connectivity: uses and interpretations. Neuroimage. 2010;52:1059–69. https://doi.org/10.1016/j.neuroimage.2009.10.003.

Almeida RF, Comasseto DD, Ramos DB, Hansel G, Zimmer ER, Loureiro SO, et al. Guanosine anxiolytic-like effect involves adenosinergic and glutamatergic neurotransmitter systems. Mol Neurobiol. 2017;54:423–36. https://doi.org/10.1007/s12035-015-9660-x.

Nunez J. Primary culture of hippocampal neurons from P0 newborn rats. Journal of visualized experiments :JoVE. 2008. doi:https://doi.org/10.3791/895

Taxt T, Storm-Mathisen J. Uptake of D-aspartate and L-glutamate in excitatory axon terminals in hippocampus: autoradiographic and biochemical comparison with gamma-aminobutyrate and other amino acids in normal rats and in rats with lesions. Neuroscience. 1984;11:79–100.

Davies LP, Johnston GA. Uptake and release of D- and L-aspartate by rat brain slices. J Neurochem. 1976;26:1007–14. https://doi.org/10.1111/j.1471-4159.1976.tb06485.x.

Debernardi R, Magistretti PJ, Pellerin L. Trans-inhibition of glutamate transport prevents excitatory amino acid-induced glycolysis in astrocytes. Brain Res. 1999;850:39–46. https://doi.org/10.1016/s0006-8993(99)02022-3.

Bellaver B, Dos Santos JP, Leffa DT, Bobermin LD, Roppa PHA, da Silva Torres IL, et al. Systemic inflammation as a driver of brain injury: the astrocyte as an emerging player. Mol Neurobiol. 2018;55:2685–95. https://doi.org/10.1007/s12035-017-0526-2.

Souza DG, Bellaver B, Hansel G, Arus BA, Bellaver G, Longoni A, et al. Characterization of amino acid profile and enzymatic activity in adult rat astrocyte cultures. Neurochem Res. 2016;41:1578–86. https://doi.org/10.1007/s11064-016-1871-7.

Prut L, Belzung C. The open field as a paradigm to measure the effects of drugs on anxiety-like behaviors: a review. Eur J Pharmacol. 2003;463:3–33. https://doi.org/10.1016/s0014-2999(03)01272-x.

Lehre KP, Levy LM, Ottersen OP, Storm-Mathisen J, Danbolt NC. Differential expression of two glial glutamate transporters in the rat brain: quantitative and immunocytochemical observations. The Journal of neuroscience : the official journal of the Society for Neuroscience. 1995;15:1835–53.

Rothstein JD, Patel S, Regan MR, Haenggeli C, Huang YH, Bergles DE, et al. Beta-lactam antibiotics offer neuroprotection by increasing glutamate transporter expression. Nature. 2005;433:73–7. https://doi.org/10.1038/nature03180.

Xiang X, Wind K, Wiedemann T, Blume T, Shi Y, Briel N, et al. Microglial activation states drive glucose uptake and FDG-PET alterations in neurodegenerative diseases. Science translational medicine. 2021;13:eabe5640. doi:https://doi.org/10.1126/scitranslmed.abe5640.

Gavillet M, Allaman I, Magistretti PJ. Modulation of astrocytic metabolic phenotype by proinflammatory cytokines. Glia. 2008;56:975–89. https://doi.org/10.1002/glia.20671.

Miyamoto S, Duncan GE, Marx CE, Lieberman JA. Treatments for schizophrenia: a critical review of pharmacology and mechanisms of action of antipsychotic drugs. Mol Psychiatry. 2005;10:79–104. https://doi.org/10.1038/sj.mp.4001556.

Stepnicki P, Kondej M, Kaczor AA. Current concepts and treatments of schizophrenia. Molecules. 2018;23. doi:https://doi.org/10.3390/molecules23082087.

Sibson NR, Dhankhar A, Mason GF, Rothman DL, Behar KL, Shulman RG. Stoichiometric coupling of brain glucose metabolism and glutamatergic neuronal activity. Proc Natl Acad Sci USA. 1998;95:316–21. https://doi.org/10.1073/pnas.95.1.316.

Scremin OU, Jenden DJ. Acetylcholine turnover and release: the influence of energy metabolism and systemic choline availability. Prog Brain Res. 1993;98:191–5. https://doi.org/10.1016/s0079-6123(08)62398-5.

Rothman DL, Sibson NR, Hyder F, Shen J, Behar KL, Shulman RG. In vivo nuclear magnetic resonance spectroscopy studies of the relationship between the glutamate-glutamine neurotransmitter cycle and functional neuroenergetics. Philos Trans R Soc Lond B Biol Sci. 1999;354:1165–77. https://doi.org/10.1098/rstb.1999.0472.

Rothman DL, Behar KL, Hyder F, Shulman RG. In vivo NMR studies of the glutamate neurotransmitter flux and neuroenergetics: implications for brain function. Annu Rev Physiol. 2003;65:401–27. https://doi.org/10.1146/annurev.physiol.65.092101.142131.

Chen AT, Nasrallah HA. Neuroprotective effects of the second generation antipsychotics. Schizophr Res. 2019;208:1–7. https://doi.org/10.1016/j.schres.2019.04.009.

Lundberg M, Curbo S, Bohman H, Agartz I, Ogren SO, Patrone C, et al. Clozapine protects adult neural stem cells from ketamine-induced

cell death in correlation with decreased apoptosis and autophagy. Bioscience reports. 2020;40. 10.1042/BSR20193156.

Bastianetto S, Danik M, Mennicken F, Williams S, Quirion R. Prototypical antipsychotic drugs protect hippocampal neuronal cultures against cell death induced by growth medium deprivation. BMC Neurosci. 2006;7:28. https://doi.org/10.1186/1471-2202-7-28.

Stanisavljevic A, Peric I, Bernardi RE, Gass P, Filipovic D. Clozapine increased c-Fos protein expression in several brain subregions of socially isolated rats. Brain Res Bull. 2019;152:35–44. https://doi.org/10.1016/j.brainresbull.2019.07.005.

Berti V, Mosconi L, Pupi A. Brain: normal variations and benign findings in fluorodeoxyglucose-PET/computed tomography imaging. PET Clin. 2014;9:129–40. https://doi.org/10.1016/j.cpet.2013.10.006.

Conley RR, Kelly DL. Management of treatment resistance in schizophrenia. Biol Psychiat. 2001;50:898–911. https://doi.org/10.1016/s0006-3223(01)01271-9.

Cohen RM, Nordahl TE, Semple WE, Andreason P, Litman RE, Pickar D. The brain metabolic patterns of clozapine- and fluphenazine-treated patients with schizophrenia during a continuous performance task. Arch Gen Psychiatry. 1997;54:481–6.

Molina V, Sanz J, Sarramea F, Palomo T. Marked hypofrontality in clozapine-responsive patients. Pharmacopsychiatry. 2007;40:157–62. https://doi.org/10.1055/s-2007-984399.

Molina V, Gispert JD, Reig S, Sanz J, Pascau J, Santos A, et al. Cerebral metabolic changes induced by clozapine in schizophrenia and related to clinical improvement. Psychopharmacology. 2005;178:17–26. https://doi.org/10.1007/s00213-004-1981-9.

Authors and Affiliations

Andréia Rocha[1] · Bruna Bellaver[1] · Débora G. Souza[1] · Guilherme Schu[1,2] · Igor C. Fontana[1] · Gianina T. Venturin[3] · Samuel Greggio[3] · Fernanda U. Fontella[1] · Manoela L. Schiavenin[1] · Luiza S. Machado[1] · Diogo Miron[4] · Jaderson C. da Costa[3] · Pedro Rosa-Neto[5,6] · Diogo O. Souza[1,7] · Luc Pellerin[8] · Eduardo R. Zimmer[1,9,10]

[1] Graduate Program in Biological Sciences: Biochemistry, Universidade Federal Do Rio Grande Do Sul, Porto Alegre, Brazil

[2] Proaction Laboratory, Faculty of Psychology and Education Sciences, University of Coimbra, Coimbra, Portugal

[3] Preclinical Research Center, Brain Institute (BraIns) of Rio Grande Do Sul, Pontifical Catholic University of Rio Grande Do Sul (PUCRS), Porto Alegre, Brazil

[4] Faculty of Pharmacy, Universidade Federal Do Rio Grande Do Sul, Porto Alegre, Brazil

[5] Translational Neuroimaging Laboratory, McGill University Research Centre for Studies in Aging, Douglas Research Institute, Le Centre intégré universitaire de santé et de services sociaux (CIUSSS) de l'Ouest-de-l'Île-de-Montréal, Montreal, Canada

[6] Department of Neurology and Neurosurgery, Psychiatry and Pharmacology and Therapeutics, McGill University, Montreal, Canada

[7] Department of Biochemistry, Universidade Federal Do Rio Grande Do Sul, Porto Alegre, Brazil

[8] Inserm U1313, Université et CHU de Poitiers, Poitiers, France

[9] Graduate Program in Biological Sciences: Pharmacology and Therapeutics, Universidade Federal Do Rio Grande Do Sul, Porto Alegre, Brazil

[10] Department of Pharmacology, Universidade Federal Do Rio Grande Do Sul, (UFRGS), 2600 Ramiro Barcelos St, Porto Alegre, RS 90035-003, Brazil